

Terahertz response of CdTe/Cd_{1-x}Mg_xTe modulation-doped multiple quantum wells

Jerzy Łusakowski^{1,2*}, Andrzej Frączak¹, Mikołaj Grymuza¹, Eryk Imos¹, Adam Siemaszko¹, Wiktoria Solarska¹, Aniela Woyciechowska¹, Maciej Zaremba¹, Rafał Zdunek¹, Krzysztof Karpierz¹, Zbigniew Adamus^{3,4}, Tomasz Słupiński^{3,4}, Tomasz Wojtowicz³

¹ Faculty of Physics, University of Warsaw, Pasteura 5, 02-093 Warsaw, Poland

² CENTERA Laboratories, Institute of High-Pressure Physics, Polish Academy of Sciences, Sokołowska 29, 01-142 Warsaw, Poland

³ International Research Centre Mag Top, Institute of Physics, Polish Academy of Sciences, Aleja Lotników 32/46, 02-668 Warsaw, Poland

⁴ Institute of Physics, Polish Academy of Sciences, Aleja Lotników 32/46, 02-668 Warsaw, Poland

Article info

Article history:

Received 15 Feb. 2023

Received in revised form 11 Mar. 2023

Accepted 11 Mar. 2023

Available on-line 18 Apr. 2023

Keywords:

Terahertz spectroscopy; Shubnikov-de Haas oscillations; modulation-doped multiple CdTe-based quantum wells.

Abstract

Terahertz (THz) transmission, photoresistance, and electrical conductivity experiments were carried out at 4.2 K on a sample with modulation-doped CdTe/Cd_{1-x}Mg_xTe multiple quantum wells. The measurements were carried out as a function of a magnetic field B up to 9 T and a radiation frequency between 0.1 and 0.66 THz. A broad minimum in the transmission curve was observed at magnetic fields corresponding to the cyclotron resonance at given THz frequency which was followed at larger fields by an oscillatory signal, periodic in B^{-1} . Shubnikov-de Haas oscillations were observed in magnetoconductivity and in photoresistance. Each of these experimental signals revealed the same electron concentration equal to $(1.01 \pm 0.03) \cdot 10^{12} \text{ cm}^{-2}$. THz spectroscopy results are compared with data obtained on a single quantum well and are discussed from the point of view of using such multiple quantum wells as THz optical elements.

1. Introduction

Studies of properties of multiple quantum wells (MQW) at terahertz (THz) frequencies seem to be carried out in the past almost exclusively on GaAs/Al_xGa_{1-x}As systems, both experimentally and theoretically [1–9].

On the other hand, modulation-doped CdTe-based quantum wells allow to observe phenomena which are difficult to study in GaAs-based systems. For example, a very strong electron – phonon interaction in CdTe allows to observe a non-linear dependence of the cyclotron resonance frequency on magnetic field at moderate fields of about 10 T [10] and to observe an influence of this interaction on the dispersion of plasmonic excitation [11]. Also, the effective electron mass higher in CdTe than in GaAs allows to use modulation-doped CdTe-based quantum wells as resonant THz detectors at higher magnetic fields [12]. Another important experimental result related to the THz spectroscopy of CdTe-based quantum structures was determination of a linear polarization of

magnetoplasmons [13] which has not been done in other materials (to the best of authors' knowledge).

In the experiments described above, samples with a single or double CdTe quantum wells were studied. Possibly, the only THz experiment carried out so far on CdTe-based MQW was application of Cd_{1-x}Mn_xTe/Cd_{1-y}Mg_yTe MQW as a material for generation of THz radiation in a time-domain spectroscopy system [14]. In the present paper, we study THz properties of CdTe-based MQW using monochromatic CW excitations and magnetic fields. The measurements allow us to compare the THz response of MQW structures with that of single CdTe-based quantum wells recently studied by our group [15].

2. Sample and experimental details

2.1. Sample: CdTe/Cd_{0.7}Mg_{0.3}Te multiple quantum wells

The sample used in the present experiment was grown using molecular beam epitaxy on (001)-oriented semi-insulating GaAs. The substrate was first covered with a 30 nm thick ZnTe nucleation layer on which 3 μm thick

*Corresponding author at: jerzy.lusakowski@fuw.edu.pl

CdTe and 3 μm thick $\text{Cd}_{0.7}\text{Mg}_{0.3}\text{Te}$ buffers were grown. The part of the sample comprising quantum wells and modulation-doped barriers consists of 10 repetitions of a sequence composed of a 20 nm thick CdTe quantum well, a 20 nm thick $\text{Cd}_{0.7}\text{Mg}_{0.3}\text{Te}$ spacer, a 4 nm thick iodine-doped $\text{Cd}_{0.7}\text{Mg}_{0.3}\text{Te}$ layer, as well as a 30 nm thick undoped $\text{Cd}_{0.7}\text{Mg}_{0.3}\text{Te}$ layer. A rectangular sample with dimensions of approximately 4 mm \times 8 mm was supplied with soldered indium contacts (the contacts were prepared by putting tiny indium flakes on the sample surface and heating them with a soldering iron). The contacts were positioned in a standard Hall cross configuration with two-bar-shaped current-supplying contacts and four drop-like contacts used for voltage measurements.

2.2. Experimental details

The experiments were carried out with the sample cooled to 4.2 K by an exchange gas. The sample was mounted at the end of a stainless-steel tube which served as an oversized waveguide for THz radiation. The diameter of the tube was 18 mm and the radiation was focused on the sample with a copper cone attached to the end of the tube. The insert allowed to illuminate the sample with a visible light. Generally, illumination of the sample at low temperatures can change slightly the concentration of a two-dimensional electron gas (2DEG) and usually essentially increases its mobility. For this reason, it is rather standard procedure to carry out measurements after illuminating the sample. In the case of the present experiments, we wanted to compare the sample properties before and after illumination with a green laser light (532 nm). For this reason, the sample was cooled in the dark, measurements were carried out, and then the sample was illuminated and the measurements were repeated. The sample was placed in the centre of a 9 T superconducting coil. A bolometer (a polished Allan-Bradley resistor) was placed below the sample which allowed to detect the intensity of a THz radiation passing through the sample. The electrical circuit of the bolometer consisted of the bolometer connected in series with a 130 k Ω resistor (while the resistance of the bolometer at 4.2 K was equal to about 100 k Ω) and a voltage source supplying the voltage equal to 5 V. The measured THz-related signal was the voltage drop on the series resistor and it was delivered to a lock-in synchronised with a mechanical chopper working at a frequency equal to 4 Hz. Such a low chopping frequency was chosen because the response time of the bolometer was long and the low chopping frequency maximized the measured signal.

The Hall effect measurements were carried out by a DC technique with a magnetic field increasing to ± 9 T. These measurements were carried out only after the sample was illuminated with the green light for about 20 h.

Transmission experiments were conducted for several values of the photon frequency in the bands around 0.1 THz, 0.33 THz, and 0.63 THz. A THz photoresistance was measured at a frequency of radiation equal to 0.336 THz. A DC current was directed to the current-supplying contacts and the photoresistance signal was given by variations of the voltage on the sample (no load resistor was used in these measurements) and measured with a lock-in at a frequency of 4 Hz (chopping frequency of the radiation beam).

3. Results

Results of 0.1 THz radiation transmission measurements are shown in Fig. 1. Data were collected before illumination with the laser, then after 10 min. and 20 h of illumination. There is a visible change between the spectra obtained before and after illumination but only a small one between the short and long illumination times which indicates that such long exposition times are not necessary. In all cases, oscillations of the transmitted signal develop at higher B values and appear to be periodic in $1/B$.

In Fig. 2, the data corresponding to transmission of radiation with few values of frequency in the band of 0.63–0.66 THz were presented. As can be seen from the inset to Fig. 2, the power of radiation changed by a factor of about 2, but the shape of the curves changed essentially and only one of these curves (at 0.6604 Hz) showed a structure corresponding to a well-defined resonance. The position of the cyclotron resonance at this frequency of radiation and the effective mass equal to $0.102m_0$ determined in Ref. 15 is 2.407 T which perfectly agrees with the position of the minimum of the green curve in Fig. 2.

Let us note that each of the presented curves was registered two times – with the magnetic field increasing to a maximum value of about 7 T and then decreasing to zero – and only minor (if any) changes in the shape of the curves were observed.

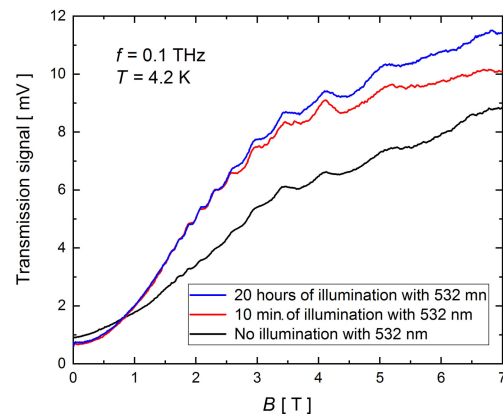


Fig. 1. The transmission signal before illumination (black), after 10 min. (red), and 20 h (blue) of illumination with a 532 nm light. Frequency of radiation was equal to 0.1 THz.

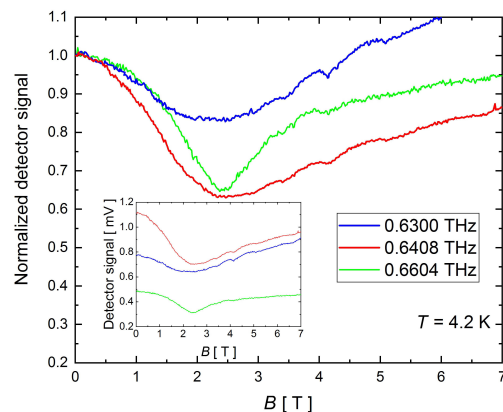


Fig. 2. Normalised spectra of transmission at 0.6300 (blue), 0.6408 (red), and 0.6604 (green) THz. The inset shows raw data.

Finally, Figure 3 shows the signal of photoresistance measured at 0.336 THz and Figure 4 presents the results of the Hall effect measurements.

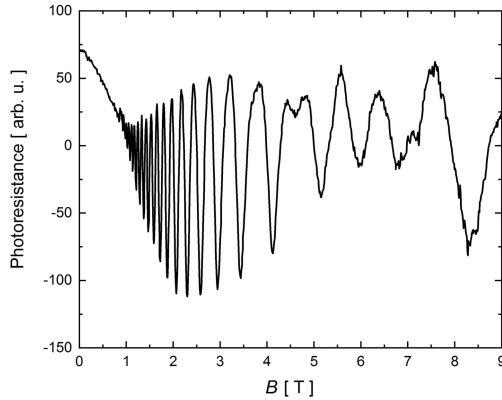


Fig. 3. Photoresistance as a function of a magnetic field at 4.2 K and a radiation frequency equal to 0.336 THz.

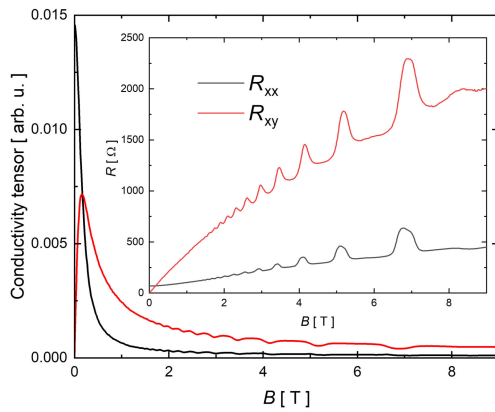


Fig. 4. Inset: longitudinal (black) and Hall (red) voltage presented as resistances. Main body: conductivity tensor: σ_{xx} (black) and σ_{xy} (red). $T = 4.2$ K.

4. Discussion

Transmission spectra obtained on this multiple-quantum-wells sample differ essentially from those obtained on a similar single quantum well [15]. In the latter case, a well-defined spectral feature was observed which was interpreted as a signature of the cyclotron resonance and allowed to determine the electron effective mass equal to $0.102m_0$. A typical width of the line was equal to about 0.2 T.

In the case of a multiple-quantum-wells structure, the transmission spectra are more difficult to interpret. First, the minima in the transmission seen in the spectra in Fig. 2 are much broader, their width is at about 1 T. The minimum is not observed in the case of 0.1 THz but this is most probably caused by the fact that the cyclotron resonance for such a low frequency would appear at about 0.36 T where the Landau quantization is not well developed as can be judged from monotonic dependencies of R_{xx} and R_{xy} in Fig. 4, and the photoresistance in Fig. 3. Generally, in view of these results, it seems impossible to determine the position of the cyclotron resonance in a reliable way.

Second, in all spectral responses presented above, an oscillatory signal appears. An analysis of these oscillations leads obviously to presenting them as a function

of B^{-1} and calculating their period. In all cases presented in Figs. 1–4, we observe the same periodicity of the oscillations which is equal to about 0.048 T^{-1} . Before discussing the origin of these oscillations let us concentrate on the results of the Hall conductivity measurements.

A standard procedure applied to voltages measured for $\pm I, \pm B$ configurations led to results presented in the inset to Fig. 4 which were subsequently recalculated to give a magnetic-field dependence of the conductivity tensor. These results allowed us to get an insight to the conductivity mechanism in the studied sample. It was noted that oscillations of the resistance which are interpreted as the Shubnikov-de Haas oscillations are visible both in R_{xx} and R_{xy} (and σ_{xx} and σ_{xy}). Let us recall that a high-quality 2DEG shows a quantum Hall effect at high magnetic fields which is marked by plateaux in the Hall resistance. Such plateau in σ_{xy} with a corresponding zero value of σ_{xx} was observed on a single CdTe/Cd_{1-x}Mg_xTe quantum well [15]. This typical shape has not been observed for the present measurements. However, such a form of the Hall resistance in samples containing nominally only a 2DEG was observed in the past, e.g., in pseudomorphic In_{0.2}Ga_{0.8}As/GaAs [16, 17] or CdTe/Cd_{1-x}Mg_xTe quantum wells [18, 19]. The reason of such a shape, and also of a parabolic background in the longitudinal resistance, is attributed to a parallel (or a parasitic) conductance, i.e., to existence of a conducting channel, other than the quantum well, which collects a big enough concentration of free electrons participating in the electrical transport. Such additional channels are often formed in the barrier, in a region of donor-doping, as it was, e.g., shown in the case of CdTe/Cd_{1-x}Mg_xTe quantum wells in Ref. 18.

The electrons which are involved in the parallel conductivity show a much lower mobility than electrons in the quantum well which is a feature allowing to separate their contributions to the total conductivity. In the range of low magnetic fields, i.e. if $\mu_i B \ll 1$, the classical conductivity tensor of a degenerate electron gas has the components described by the equations

$$\sigma_{xx} = \sum_i \frac{n_i e \mu_i}{1 + \mu_i^2 B^2},$$

$$\sigma_{xy} = \sum_i \frac{n_i e \mu_i^2 B}{1 + \mu_i^2 B^2},$$

where the index i numbers the groups of carriers with mobility μ_i and concentration n_i . In the present work, $i = 1$ represents electrons in the quantum wells and $i = 2$ represents these responsible for the parallel conductivity.

The above equations show that σ_{xx} changes faster for high- than for low-mobility carriers, whereas σ_{xy} should be much smaller for low-mobility than high-mobility carriers if this difference is not overcompensated by the concentration ratio. This observation leads to different models applied to describe a conductivity tensor in the case of many carrier conductivity. First, the most direct method is to fit a four-parameter model described by (1) and (2) to experimental data. Second, if the assumption $\mu_1 \gg \mu_2$ is justified, then it can be assumed that carriers in the parasitic channel contribute with a constant (i.e., magnetic field – independent) component to σ_{xx} (1) and do not contribute at

all to σ_{xy} (2). This approach was adopted by Wasik *et al.* [18, 19] in their analysis of the conductivity tensor in samples with one CdTe/Cd_{1-x}Mg_xTe quantum well. In a more advanced form, it was also used to describe the conductivity tensor in a semi-insulating GaAs under conditions of carrier localisation by long-range fluctuations of the electrostatic potential [20].

When the mobility of carriers and the magnetic field are high enough, Landau quantization leads to the Shubnikov-de Haas oscillations and possibly – in the case of 2D systems – to the quantum Hall effect. The period of oscillations presented as a function of the inverse of magnetic field (Δ) allows to estimate a 2D concentration of electrons, n_{2D} [21]

$$\Delta = \frac{2e}{hn_{2D}}.$$

However, an oscillatory form of magnetoconductivity is also present in the case of a degenerate 3D electron gas and then a relation between the period Δ and the bulk concentration n_{3D} is [22]

$$\Delta = \frac{2e}{h} \left(\frac{8}{9\pi} \right)^{1/3} \frac{1}{n_{3D}^{2/3}}.$$

An experimental method to determine whether low-mobility electrons effectively form a 2D or a 3D parasitic channel is based on carrying out magnetoconductivity experiments with the sample tilted with respect to the direction of the magnetic field. This type of conductivity measurements has recently acquired a special interest in the context of topological insulators where separation of 2D and 3D conducting channels is of the basic importance (see, e.g., [23]). A more precise estimation of low- and high-mobility electrons contribution to the conductivity tensor requires measurements at high magnetic field when one could observe the changes σ_{xx} and σ_{xy} related to low-mobility carriers. Such procedure was successfully applied, for example, in the case of a room-temperature conductivity in a GaN/AlGaIn heterostructure [24].

The periodicity in traces presented in Figs. 1–4, equal to 0.048 T⁻¹, leads to a 2D electron concentration equal to 10¹² cm⁻² [see (3)]. An analysis of a non-oscillatory part of the conductivity tensor (below 2 T, see Fig. 4) was carried out with a four-parameter fitting to give $n_1 = 1.4 \cdot 10^{12}$ cm⁻², $\mu_1 = 61\,000$ cm²/Vs and $n_2 = 4.1 \cdot 10^{11}$ cm⁻², $\mu_2 = 5600$ cm²/Vs. Almost identical set of parameters was obtained fitting (1) and (2) to data in a full range of the magnetic field, up to 9 T.

A three-parameter fitting, assuming no contribution to σ_{xy} from the low-mobility carriers [18, 19] gives $n_1 = 1.5 \cdot 10^{12}$ cm⁻², $\mu_1 = 60\,000$ cm²/Vs and $n_2\mu_2 = 1.3 \cdot 10^{15}$ 1/Vs while in the four-parameter fitting $n_2\mu_2 = 2.3 \cdot 10^{15}$ 1/Vs.

These two models give consistent results in the case of the high-mobility electrons and approximately agree in the case of low-mobility electrons. On the other hand, concentration n_1 is essentially higher than that determined from the periodicity of the Shubnikov-de Haas oscillations which means that the concentration of high-mobility electrons determined at low magnetic fields disagrees with

that determined at high B . A possible reason for this discrepancy could be a magnetic-field-induced freeze-out of electrons at localised levels at high B [25], but clearly measurements at high B and with a tilt of sample are recommended before putting forward a more definite hypothesis.

Data referring to a THz response of the sample, presented in Figs. 1–3 show the same periodicity in B^{-1} as the conductivity tensor which means that the THz response of the sample is related to free electrons. As can be observed from the shape of presented curves, the response is not limited to the cyclotron resonance but also involves a non-resonant process. A non-resonant absorption on free electrons in quantizing magnetic fields was studied in the past both theoretically and experimentally (see, e.g., [26]) and we propose that it is responsible (together with reflectivity) for the shape of transmission curves presented above. The oscillatory character would just reflect changes of the density of states at the Fermi level which mark the energetic position of electrons that could be heated by low-energy photons of THz radiation used in the experiment.

As it is seen in Fig. 2, the shape of transmission curves cannot be considered as well-defined for given frequency of radiation, because it changes with its power. Also, the minimum in absorption curves which mark the position of the cyclotron resonance in samples with only one quantum well [15] is very broad. Although it could be assume that the quantum wells are not exact mutual copies, there is no reason to expect an essential broadening of the cyclotron resonance (with relation to a single quantum well) just because of an increased number of wells. A more detailed study of the shape of the transmission curves is necessary with application of more energetic photons which could shift the resonance position to higher magnetic fields when the separation between Landau levels is more visible.

5. Conclusions

In conclusion, the THz spectroscopy (transmission and photoresistance) and the Hall effect measurements on a sample containing 10 modulation-doped CdTe quantum wells with Cd_{0.7}Mg_{0.3}Te barriers were conducted. Measurements were carried out at 4.2 K with the magnetic field up to 9 T. A very broad signature of the cyclotron resonance was observed which practically excluded the possibility to determine the exact position of this resonance. Transmission and photoresistance curves showed the same regular periodicity in B^{-1} which allowed to determine the electron concentration. This concentration was by 50% lower than that determined by fitting a low- B conductivity tensor formula to a non-oscillatory part of the tensor components. Suggestions of further experiments which could resolve these discrepancies are given which involve measurements at higher and tilted magnetic field and a higher energy of THz photons.

Authors' statement

Research concept, data collection and treatment, writing the article: J.L.; data collection: A.F., M.G., E.I., A.S., W.S., A.W., M.Z., A.Z., K.K, and Z.A.; growth of samples: T.S. and T.W.

Acknowledgements

This research was partially supported by the Polish National Science Centre grant UMO-2019/33/B/ST7/02858 and by the Foundation for Polish Science through the IRA Programme co-financed by EU within SG OP (Grant No. MAB/2017/1).

References

- [1] Cheng, J.-P., McCombe, B. D. & Brozak, D. Impurity-bound magnetopolarons in confined structures. *Surf. Sci.* **267**, 488 (1992). [https://doi.org/10.1016/0039-6028\(92\)91183-C](https://doi.org/10.1016/0039-6028(92)91183-C)
- [2] Cheng, J.-P., McCombe, B. D., Brozak, G. & Schaff, W. Resonant electron – optical phonon interactions for impurities in GaAs and GaAs/Al_xGa_{1-x}As quantum wells and superlattices. *Phys. Rev. B* **48**, 17243 (1993). <https://doi.org/10.1103/PhysRevB.48.17243>
- [3] Ashkinadze, B. M., Cohen, E., Ron, A. & Pfeiffer, L. Microwave modulation of exciton luminescence in GaAs/Al_xGa_{1-x}As quantum wells. *Phys. Rev. B* **47**, 10613–10618 (1993). <https://doi.org/10.1103/physrevb.47.10613>
- [4] Ryu, S. R., Jiang, Z. X., Li, W. J., McCombe, B. D. & Schaff, W. Observation of *D* triplet transitions in GaAs/Al_xGa_{1-x}As multiple quantum wells. *Phys. Rev. B* **54**, R11086 (1996). <https://doi.org/10.1103/PhysRevB.54.R11086>
- [5] Celik, H., Cankurtaran, M., Bayrakli, A., Tiras, E. & Balkan, N. Well-width dependence of the in-plane effective mass and quantum lifetime of electrons in GaAs/Al_xGa_{1-x}As multiple quantum wells. *Semicond. Sci. Technol.* **12**, 389–395 (1997). <https://yunus.hacettepe.edu.tr/~hucelik/PDF/10.pdf>
- [6] Heron, R. J. et al. Far-infrared laser photoconductivity of n-GaAs multiple quantum wells in a pulsed magnetic field. *Physica B* **246–247**, 290–293 (1998). [https://doi.org/10.1016/S0921-4526\(97\)00918-6](https://doi.org/10.1016/S0921-4526(97)00918-6)
- [7] Kozhevnikov, M., Cohen, E., Ron, A. & Shtrikman, H. Electron and hole microwave cyclotron resonance in photoexcited undoped GaAs/Al_xGa_{1-x}As multiple quantum wells. *Phys. Rev. B* **60**, 16885 (1999).
- [8] Kim S.-W. et al. Optical properties of magnetoplasmons in multiple quantum wells. *Physica B Condens Matter.* **322**, 12–23 (2002). [https://doi.org/10.1016/S0921-4526\(02\)00591-4](https://doi.org/10.1016/S0921-4526(02)00591-4)
- [9] Zybert, M. et al. Landau levels and shallow donor states in GaAs/AlGaAs multiple quantum wells at megagauss magnetic fields. *Phys. Rev. B* **95**, 115432 (2017). <https://doi.org/10.1103/PhysRevB.95.115432>
- [10] Grigelionis, I. et al. Terahertz magneto-spectroscopy of a point contact based on CdTe/CdMgTe quantum well. *Proc. SPIE* **9199**, 91990G (2014). <https://doi.org/10.1117/12.2061938>
- [11] Grigelionis, I. et al. Magnetoplasmons in high electron mobility CdTe/CdMgTe quantum wells. *Phys. Rev. B* **91**, 075424 (2015). <https://doi.org/10.1103/PhysRevB.91.075424>
- [12] Yavorskiy, D. et al. Grating metamaterials based on CdTe/CdMgTe quantum wells as terahertz detectors for high magnetic field applications. *Appl. Sci.* **10**, 2807 (2020). <https://doi.org/10.3390/app10082807>
- [13] Yavorskiy, D. et al. Polarization of magnetoplasmons in grating metamaterials based on CdTe/CdMgTe quantum wells. *Materials* **13**, 1811 (2020). <https://doi.org/10.3390/ma13081811>
- [14] Rungsawang, R. et al. Terahertz radiation from magnetic excitations in diluted magnetic semiconductors. *Phys. Rev. Lett.* **110**, 177203 (2013). <https://doi.org/10.1103/PhysRevLett.110.177203>
- [15] Łusakowski, J. et al. Magneto-spectroscopy of CdTe/Cd_{1-x}Mg_xTe modulation-doped quantum wells in THz and visible range. *Opto-Electron. Rev.* (accepted).
- [16] Li, G., Babiński, A. & Jagadish, C. Subband electron densities of Si δ-doped pseudomorphic In_{0.2}Ga_{0.8}As/GaAs heterostructures. *Appl. Phys. Lett.* **70**, 3582 (1997). <https://www.fuw.edu.pl/~babinski/Publications/apl703582.pdf>
- [17] Babiński, A., Li, G. & Jagadish, C. The persistent photoconductivity effect in modulation Si δ-doped pseudomorphic In_{0.2}Ga_{0.8}As/GaAs quantum well structure. *Appl. Phys. Lett.* **71**, 1664 (1997). <https://doi.org/10.1063/1.119788>
- [18] Wasik, D. et al. Parasitic conduction phenomena in modulation doped CdTe/CdMgTe: I heterostructures grown on GaAs substrates. *J. Appl. Phys.* **91**, 753 (2002). <https://doi.org/10.1063/1.1426233>
- [19] Wasik, D. et al. Elimination of parallel transport in modulation-doped CdTe/CdMgTe: I heterostructures. *Phys. Status Solidi B Basic Res.* **229**, 183 (2002). [https://doi.org/10.1002/1521-3951\(200201\)229:1<183::AID-PSSB183>3.0.CO;2-O](https://doi.org/10.1002/1521-3951(200201)229:1<183::AID-PSSB183>3.0.CO;2-O)
- [20] Łusakowski, J. & Łusakowski, A. Magnetoconductivity and potential fluctuations in semi-insulating GaAs. *J. Phys. Condens. Matter.* **16**, 2661 (2004). <https://doi.org/10.1088/0953-8984/16/15/017>
- [21] Davies, J. H. The Physics of Low-Dimensional Semiconductors. An Introduction. Chapter 6 (Cambridge University Press, 1998).
- [22] Nag, B. R. *Electron Transport in Compound Semiconductors. Chapter 10* (Verlag Berlin, Heidelberg, New York, 1980).
- [23] Cao, H. et al. Quantized Hall effect and Shubnikov-de Haas oscillations in highly doped Bi₂Se₃: Evidence for layered transport of bulk carriers. *Phys. Rev. Lett.* **108**, 216803 (2012). <https://doi.org/10.1103/PhysRevLett.108.216803>
- [24] Skierbiszewski, C. et al. High mobility two-dimensional electron gas in AlGa_N/Ga_N heterostructures grown on bulk Ga_N by plasma assisted molecular beam epitaxy. *Appl. Phys. Lett.* **86**, 102106 (2005). <https://doi.org/10.1063/1.1873056>
- [25] Dyakonov, M. I., Efros, A. L. & Mitchell, D. L. Magnetic freeze-out of electrons in extrinsic semiconductors. *Phys. Rev.* **180**, 813 (1969). <https://doi.org/10.1103/PhysRev.180.813>
- [26] Wu, C. C., Tsai, J. & Lin, C. J. Free-carrier absorption in n-type gallium – arsenide in quantizing magnetic fields. *Phys. Rev. B* **43**, 7328 (1991). <https://doi.org/10.1103/PhysRevB.43.7328>